

# Generative Data Mining with Longtail-Guided Diffusion

David S. Hayden<sup>1</sup> Mao Ye<sup>1</sup> Timur Garipov<sup>2</sup> Gregory P. Meyer<sup>1</sup> Carl Vondrick<sup>3</sup> Zhao Chen<sup>4</sup> Yuning Chai<sup>5</sup>  
Eric Wolff<sup>1</sup> Siddhartha S. Srinivasa<sup>1</sup>

## Abstract

It is difficult to anticipate the myriad challenges that a predictive model will encounter once deployed. Common practice entails a *reactive*, cyclical approach: model deployment, data mining, and retraining. We instead develop a *proactive* longtail discovery process by imagining additional data during training. In particular, we develop general model-based longtail signals, including a differentiable, single forward pass formulation of epistemic uncertainty that does not impact model parameters or predictive performance but can flag rare or hard inputs. We leverage these signals as guidance to generate additional training data from a latent diffusion model in a process we call Longtail Guidance (LTG). Crucially, we can perform LTG without retraining the diffusion model or the predictive model, and we do not need to expose the predictive model to intermediate diffusion states. Data generated by LTG exhibit semantically meaningful variation, yield significant generalization improvements on image classification benchmarks, and can be analyzed to proactively discover, explain, and address conceptual gaps in a predictive model.

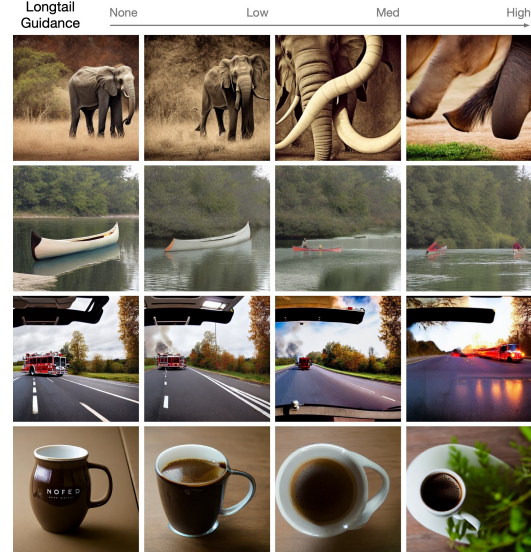


Figure 1. Diffusion with Longtail Guidance (LTG) generates synthetic data that are difficult or rare for an existing predictive model. The predictive model can then a) be fine-tuned on this data to improve generalization performance, or b) the synthetic data can be analyzed to understand conceptual gaps in the predictive model. Guided generations exhibit more extreme views and lighting compared to unguided generations.

## 1. Introduction

Longtail encounters are common in production ML systems but difficult to anticipate and be robust towards. Recently, the answer has been: add more training data and more compute (Kaplan et al., 2020). However, the time and cost to acquire additional data, especially longtail data, can be prohibitive (e.g. train instances occurs 1 time for every  $10^4$  car instances in Berkeley DeepDrive (Yu et al., 2020)). Additional compute can be traded for improved performance; see distillation (Yu et al., 2023b; Gou et al., 2021) and synthetic data generation (Du et al., 2024; Zhang et al., 2023b) for

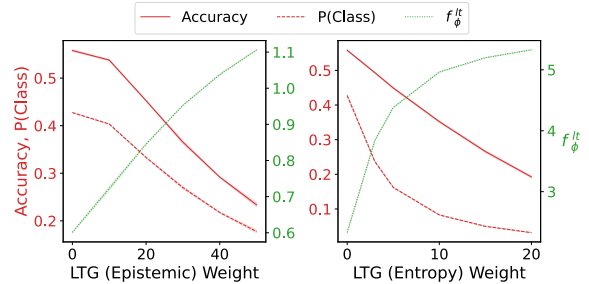


Figure 2. Predictive model performance (left axis, red) and model-based longtail signals  $f_{\phi}^{lt}$  (right axis, green) on synthetic data generated by varying Longtail Guidance weights for two types of longtail signals: Epistemic (left plot) and Entropy (right plot). In all cases, guided synthetic data generations exhibit lower correct class probability, lower accuracy, and higher longtail signals compared to unguided generations (guidance weight 0).

<sup>1</sup>Cruise, LLC, San Francisco, CA <sup>2</sup>OpenAI, San Francisco, CA <sup>3</sup>Columbia University, New York, NY <sup>4</sup>Upwork, Palo Alto, CA <sup>5</sup>Meta, Menlo Park, CA. Correspondence to: David Hayden <david.hayden@getcruise.com>.

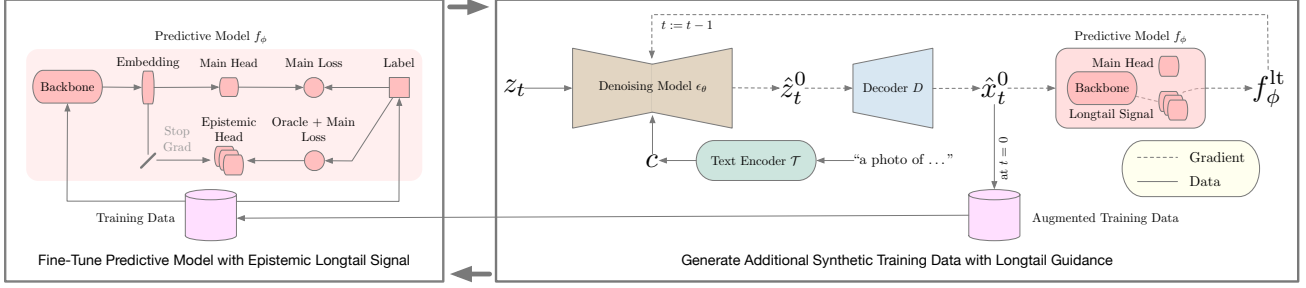


Figure 3. In Longtail Guidance, we iteratively fine-tune existing predictive model  $f_\phi$  with longtail signal  $f_\phi^{\text{lt}}$  (left) then freeze model weights  $\phi$  and generate synthetic data with latent diffusion model  $\epsilon_\theta$  guided by  $f_\phi^{\text{lt}}$  that is, by definition, rare or disproportionately hard for  $f_\phi$  (right). Synthetic data are added to  $f_\phi$ 's training set, and the process repeats.

offline approaches, chain of thought (Yao et al., 2024; Wei et al., 2022) for online approaches. While online approaches show promise, they are not applicable to real-time, safety-critical systems such as autonomous driving, which have strict parameter count and inference latency budgets.

Production ML systems are iteratively developed in a continuous, reactive cycle of: collect data, deploy model, encounter longtail edge cases, repeat. We wish to expedite this cycle and move it towards a proactive approach of longtail discovery. Existing offline approaches appeal to larger models (knowledge distillation, synthetic data generation) or summarize training data (data distillation). Yet, they do not directly account for what is rare or difficult for an existing, currently-deployed predictive model.

We wish to trade additional offline compute for performance by generatively mining additional training data that is hard or rare *from the perspective of an existing predictive model*. Distinct from adversarial training and robustness approaches (Bansal & Grover, 2023; Zhang et al., 2022a; Goyal et al., 2021; Hendrycks et al., 2021) which imbue models with invariance to distribution shift or small, often imperceptible changes, we wish to generate semantically meaningful, in-distribution examples that cause high model uncertainty.

Foundation generative models such as Stable Diffusion (Rombach et al., 2022), Pixart (Chen et al., 2025), GPT (Brown et al., 2020; OpenAI, 2023), and Claude (Anthropic, 2024) are exposed to Internet-scale data, but it is not obvious how to use them to generate data that is specifically challenging to an existing predictive model. We seek to explicitly couple the vast knowledge contained in foundation generative models with the specific challenges faced by an *existing* predictive model. But how can we ensure that the generative model produces data that is relevant (has meaningful learning signal) to a given predictive model? Existing approaches, like prompt tuning and reasoning in an embedding space (such as CLIP) (Zhang et al., 2023b; Du et al., 2024) can generate synthetic data that improves model generalization performance up to a point, but they do not condition on the deployed model.

Following, we develop model-based longtail signals (Section 2), including a lightweight Epistemic Head (Section 2.1), that effectively indicate an example as being hard or rare while keeping the original predictive model intact. We then develop Longtail Guidance (Section 3), a simple method for coupling Internet-scale knowledge in diffusion models with the specific struggles of an existing predictive model. We show that synthetic data produced with Longtail Guidance yields outsized generalization improvements over existing synthetic data generation approaches and that these synthetic data exhibit semantically meaningful variations, including occlusion and extreme views, see Figures 1, 2, 6 and Section 4 for comparisons. In summary, we contribute:

1. Epistemic Head: a differentiable, single forward-pass formulation of epistemic uncertainty that does not impact existing model weights or performance, detects rare or hard examples, and guides data generation towards high-value training examples.
2. Longtail Guidance (LTG): a latent diffusion guidance technique that generates high-value, difficult and/or rare training examples from the perspective of an existing predictive model. It requires no changes in training for the diffusion model or the predictive model.
3. Longtail Introspection: through VLM analysis of LTG-generated data, we find keywords describing what an existing predictive model struggles with. Keywords can be used to prompt diffusion models for high-value data or to inform future data collection.

## 2. Model-Based Longtail Signals

Longtail is a *suitcase word* (Minsky, 2006) – it does not have a single definition. Two reasonable definitions include:

- **Rare:** An input is longtail if instances similar to it are rare in training data. This definition naturally captures a data-centric view in which events are longtail if their overall occurrence is rare (independent of any model).

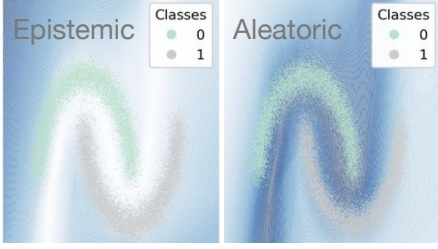


Figure 4. Epistemic  $E(y, \phi)$  vs aleatoric  $\mathbb{E}_\phi[\mathcal{U}(y | \phi)]$  uncertainty. Epistemic increases with distance from the data manifold. Aleatoric increases with proximity to the decision boundary.

- **Hard:** An input is longtail if it is disproportionately difficult for a given model to correctly reason about.

We develop differentiable model-based longtail signals that can flag both rare and hard instances. We then use model-based longtail signals offline to generate additional longtail synthetic training data that provide outsized generalization improvements. Following, we introduce the Epistemic Head, a lightweight addition to any predictive model that does not impact predictive performance but provides superior longtail signals based on detecting hard or rare examples.

We wish to develop longtail signals that are general to loss, architecture (transformer, convolutional), or output space (discrete, continuous). Ideally, they do not affect model performance or require changes to model training. Obvious candidates would be an uncertainty measure of the output, such as entropy or variance. Others can be gathered from the anomaly and out-of-distribution detection literature. One is the Helmholtz free energy, defined as the negative log partition function of an energy model  $p(y | x)$ ,

$$E(x) = -T \log \int_{y'} e^{E(x, y')/T} dy' \quad (1)$$

where  $x$  is some input with energy  $y$ . This energy can be computed in typical classification models as the negative, temperature-scaled log-sum-exp of the logits,  $E(x) = -T \log \sum_i e^{f_i(x)/T}$  where  $f_i(x)$  is the  $i^{\text{th}}$  logit of a predictive model  $f(x)$  that forms a probability distribution by softmax. Energy was shown to be effective in discriminating in-distribution and out-of-distribution data (Liu et al., 2020). Like entropy and variance, it requires no model adjustment or retraining. We use entropy and energy as baselines.

## 2.1. Epistemic Head

Traditional measures of predictive uncertainty, like entropy, do not distinguish what is rare from what is ambiguous or hard. To address longtail scenarios, we would ideally account for both. To do so, we decompose predictive uncertainty into two components: epistemic and aleatoric (Figure 4). For test input  $x$  with unknown label  $y$  and predictive

model parameters  $\phi$  drawn from distribution  $\Phi$ , epistemic uncertainty is defined as (Depeweg et al., 2018),

$$E(y, \Phi) = \mathcal{U}(y) - \mathbb{E}_\phi[\mathcal{U}(y | \phi)] \quad (2)$$

where we implicitly condition on  $x$  in each term, and where  $\mathcal{U}$  is an uncertainty measure, such as entropy for discrete  $y$  or variance for continuous  $y$ . If entropy, Eqn 2 is equivalent to measuring the mutual information between parameter distribution  $\Phi$  and unknown target  $y$ , which informs us about how much knowing about one tells us about the other.

In principle, epistemic uncertainty can be computed by sampling from the posterior predictive distribution:

$$p(y | x) = \int p(y | \phi, x) p(\phi | x_{\text{train}}, y_{\text{train}}) d\phi. \quad (3)$$

The first term is a likelihood for test label  $y$  and the second term is a posterior distribution for model parameters  $\phi$ , conditioned on all previous training data  $(x_{\text{train}}, y_{\text{train}})$ .

Performing the inference required to sample from Eqn 3 is intractable for modern neural networks. Nevertheless, it can be approximated. One approach is variational inference, typified by Monte Carlo dropout (Gal & Ghahramani, 2016), where the same input is passed through a network many times (often 50 or more forward passes), with test time variation in each pass enabled by random Bernoulli dropout. Unfortunately, this would be expensive to compute and is not conveniently differentiable due to discrete sampling (Jang et al., 2016). It is also bested in practical terms by a model ensemble, where a small number of models, often 3 – 5, are trained (independently (Lakshminarayanan et al., 2017) or otherwise (Maddox et al., 2019)). However, computing a gradient (which we will need to generate longtail synthetic data) across  $K$  instances of a model introduces substantial memory overhead and compute latency.

In Figure 3 (left), we introduce a lightweight ensembling technique called the Epistemic Head, which provides a superior longtail signal with no impact on model performance and negligible changes to model parameter count, training time, and inference time (see Supplement A.6). Inspired by LoRA (Hu et al., 2021) and the Hydra architecture (Tran et al., 2020), we duplicate the head of an existing prediction model  $K$  times and jointly train with the same loss as the base model but with diversity encouraged through an oracle loss (Guzman-Rivera et al., 2012) that only propagates per-example loss through the best-performing head. Head outputs act as fixed-point samples from the posterior predictive (Eqn 3) under a prior determined by weight initialization and permit differentiable computation of longtail signals in a single forward pass, including  $E(y, \Phi)$ ,

$$f_\phi^h(x) \approx \mathcal{U} \left( \frac{1}{K} \sum_k p(y | \phi_k) \right) - \frac{1}{K} \sum_k \mathcal{U}(p(y | \phi_k)). \quad (4)$$

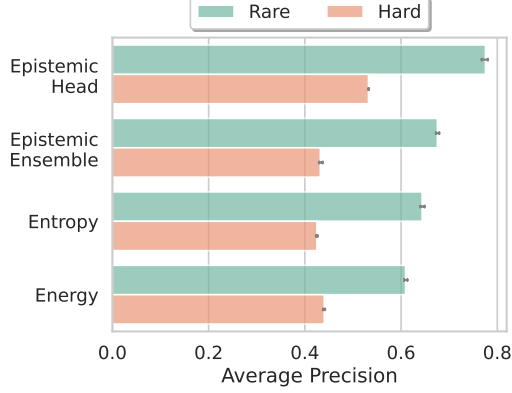


Figure 5. The Epistemic Head is a better indicator of rare or hard ImageNet-LT validation examples than entropy, energy, or epistemic signals from an independently-trained ensemble.

Base model performance is protected by a stop-grad at training time so that, similar to LoRA (Hu et al., 2021), the Epistemic Head does not impact existing model weights. In Figure 5, we demonstrate that longtail signals from the Epistemic Head more effectively indicate rare or hard examples than do entropy or energy. In particular, we train ViT-B ImageNet-LT classifiers according to (Xu et al., 2023) and compare how well our proposed longtail signals (entropy, energy, epistemic) detect rare or hard test examples. Examples are defined as rare if they come from a longtail class. Examples are defined as hard if the model incorrectly predicts the label. In Supplement A.7, we further show that detected examples are disproportionately hard.

### 3. Longtail Guidance

To motivate Longtail Guidance, we briefly review diffusion. Diffusion models learn a continuous data distribution  $p_\theta(x_0) = \int p_\theta(x_{0:T}) dx_{1:T}$  from a finite set of data samples by defining a forward noising process  $q(x_{1:T}|x_0)$  over latent states  $x_{1:T}$ , and learning a reverse denoising process  $p_\theta(x_{0:T})$ . In the DDPM (Ho et al., 2020) and DDIM (Song et al., 2020a) formulations, the forward process is a Markov chain that iteratively add noise according to schedule  $\alpha_{1:T}$  that decreases over steps  $1, \dots, T$ ,

$$q(x_t|x_{t-1}) = N(\sqrt{\alpha_t}x_{t-1}, (1 - \alpha_t)I) \quad (5)$$

However, they differ in the learned reverse process: DDPM models it as a Markov chain,

$$p_\theta(x_t|x_{t-1}) = N(\mu_\theta(x_t, t), \Sigma_\theta(x_t, t)) \quad (6)$$

where, by reparameterization for numerical stability, the diffusion network  $\epsilon_\theta(x_t, t)$  learns to predict the previously-sampled noise at each step rather than the process mean. In DDIM, the reverse process is instead modeled as non-Markovian. At each step, it predicts,

$$x_{t-1} = \sqrt{\alpha_{t-1}}\hat{x}_0^{(t)} + v_t + \sigma_t\epsilon_t \quad (7)$$

for terminal state estimate  $\hat{x}_0^{(t)}$ , directional vector  $v_t$  pointing towards  $x_t$ , and sampled noise  $\epsilon_t \sim N(0, I)$ ,

$$\hat{x}_0^{(t)} = \alpha_t^{-0.5} (x_t - \sqrt{1 - \alpha_t}\epsilon_\theta(x_t, t)) \quad (8)$$

$$v_t = (1 - \alpha_{t-1} - \sigma_t^2)^{1/2}\epsilon_\theta(x_t, t). \quad (9)$$

SDE formulations of diffusion (Song et al., 2020b) generalize DDPM and DDIM. Denoising models can be learned in one framework (DDPM) and sampled in another (DDIM).

As stated, diffusion models sampled according to Eqns 6, 7 are unconditional; they will sample instances that are distributed approximately according to the data. This can be changed with guidance. In classifier-free guidance (Ho & Salimans, 2022), the diffusion model is trained on pairs  $(x, c)$  for data  $x$  and conditioning vector  $c$  (for example, class labels or CLIP-encoded text). In contrast, classifier guidance (Dhariwal & Nichol, 2021) can be used during the sampling process even when no conditioning information was available at diffusion training time. It operates by biasing the denoising estimate in the direction of the gradient of a differentiable signal,  $\nabla f(x_t, t)$ ,

$$\hat{\epsilon}_t = \epsilon_\theta(x_t, t) - w\nabla_{x_t}f(x_t, t)\sigma_t. \quad (10)$$

Commonly,  $f(x_t, t) = \log p(y_i | x_t, t)$ , the log probability of class  $i$  under trained classifier  $f_{\phi'}$ . But this only works if classifier  $f_{\phi'}$  is trained on intermediate noisy diffusion states  $x_{1:T}$  and accepts denoising step  $t$  (thus, it trains on triples of (noisy data  $x_t$ , step  $t$ , and label  $y$ ) instead of a standard formulation of (clean data  $x$  and label  $y$ )). Training  $f_{\phi'}$  on intermediate diffusion states is required because the distribution of  $x_t$  differ from the original data  $x$ . Classifier-free guidance can be combined with classifier guidance.

Using classifier guidance to generate synthetic data in the longtail of an existing production model  $f_\phi$ , as defined by model-based longtail signal  $f_\phi^{\text{lt}}(x)$  is appealing because it can be applied to existing diffusion models without re-training. However, as stated, classifier guidance presents a dilemma: we must either fine-tune a noise-aware model  $f_{\phi'}(x_t, t)$  from the original model  $f_\phi(x)$  on noisy, intermediate diffusion states, at which point  $f_{\phi'}$  no longer reflects the production model performance of  $f_\phi$ , or we must deploy a production model  $f_{\phi'}$  that wastes capacity on intermediate diffusion states that it will not encounter in production.

There is an additional challenge with using classifier guidance for longtail data generation: SOTA diffusion models perform training and sampling in a lower dimensional latent space  $\mathcal{Z}$  by first encoding the original data using a pretrained VAE, noising (at training) and denoising (at inference) among latent states  $z_{0:T}$ , then decoding the final result back to data space  $\mathcal{X}$ . How can we pass latent  $z_t$  through production model  $f_\phi$  when it operates in data space  $\mathcal{X}$ ?

With Longtail Guidance, we find a simple diffusion guidance approach that couples longtail signals from an existing



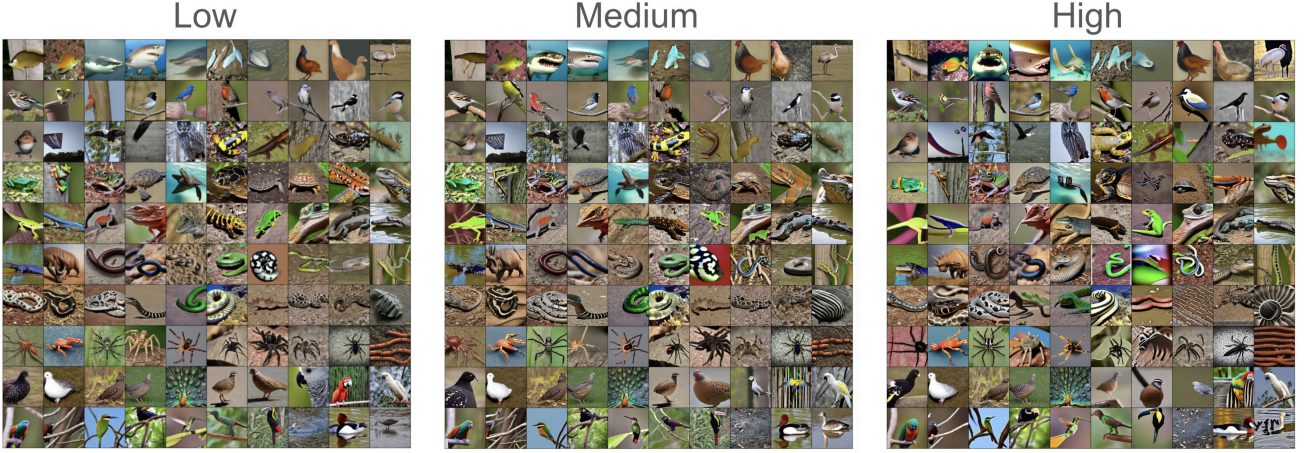


Figure 6. Synthetic data generated for 100 ImageNet classes with increasing Longtail Guidance strength, guided by a SOTA ViT ImageNet-LT classifier  $f_\phi$ . Views frequently become more extreme, occluded, or cut off. They also become more difficult for  $f_\phi$  (see Figure 2)

---

**Algorithm 1:** Longtail Guidance

---

**Input :** Latent diffusion model  $\epsilon_\theta(z_t, t)$ , predictor  $f_\phi(x)$   
decoder  $D$ , noise schedule  $\sigma_{1:T}$ , weight  $w$

**Initialize:**  $z_T \sim \mathcal{N}(0, I)$ ;

**for**  $t = T - 1, \dots, 0$  **do**

Estimate terminal latent state  $\hat{z}_t^0 = P(z_t)$  as in  
Eqn. 8;  
Decode terminal data state:  $\hat{x}_t^0 = D(\hat{z}_t^0)$ ;  
Compute model longtail signal  $f_\phi^{\text{lt}}(\hat{x}_t^0)$  as in Eqn. 4;  
Bias denoising estimate as in Eqn. 11  
Compute  $z_{t-1}$  as in Eq. 7;

**return**  $x = D(z_0)$ ;

---

production model to the Internet-scale knowledge of a latent diffusion model. Surprisingly, it requires no retraining of either the diffusion model or the production model and, in particular, it does not require the production model to be trained on intermediate diffusion states or time-conditioned inputs, as is common in Classifier Guidance.

The key idea in Longtail Guidance (LTG) is that we can differentiably estimate a terminal latent state  $\hat{z}_t^0 = P(z_t)$  with appropriate diffusion samplers (including DDIM), decode to an estimated terminal data state  $\hat{x}_t^0 = D(\hat{z}_t^0)$ , compute longtail signal  $f_\phi^{\text{lt}}(\hat{x}_t^0)$  from the existing production model (that has only ever seen real production data), and then bias the denoising estimate (in latent space) in the direction of higher production model longtail signal (See Figure 3 and Algorithm 1 for complete details):

$$\hat{\epsilon}_t = \epsilon_\theta(z_t, t) - w \nabla_{z_t} f_\phi^{\text{lt}}(D(P(z_t))) \sigma_t. \quad (11)$$

It is unintuitive that LTG would work since production model  $f_\phi$  has only ever trained on clean (data, label) pairs, not intermediate diffusion states. Empirically, however, we

find that we can generate synthetic data for which production model  $f_\phi$  exhibits lower probability of the correct class, lower accuracy, and higher longtail signal. And so long as we do not adjust the longtail guidance weight  $w$  too high, the diffusion model reliably generates data that adheres to the expected class label. Figures 1, 6 and Supplement A.10 (high-res) show example longtail synthetic ImageNet data using a SOTA ViT model (Xu et al., 2023) for guidance. Figure 2 quantitatively analyzes model performance and longtail signals on LTG-guided synthetic data generation over multiple runs of  $24k$  generations spanning all ImageNet classes. Notably, the probability of the expected class can be decreased to one-half or even one-third of its original value (from the perspective of production model  $f_\phi$ ), while staying in-distribution (as evidenced by generalization improvements in Section 4) and the model longtail signal can be more than doubled over baseline (unguided) synthetic data generation. Qualitatively, LTG data exhibit semantically meaningful changes, including more extreme, occluded, or cut off views.

Longtail Guidance is similar to Universal Guidance (Bansal et al., 2023) in that both perform differentiable decoding of latent states (see also (Jiang et al., 2023)). However, Universal Guidance is significantly more expensive and fails to remain in-distribution when guided by model-based longtail signals. In particular, Universal Guidance performs so-called recurrent and backward sampling passes, where recurrent sampling permits each diffusion step to refine its denoising estimate (each time computing a costly gradient) and each backward pass optimizes an objective (within each denoising and recurrent iterate, itself requiring multiple optimization iterates). See Figure 7 for direct comparison.

Although Longtail Guidance is not the first approach to use the predicted, decoded terminal state  $D(P(x_t))$ , we uniquely (to our knowledge) show in Supplement A.8 why

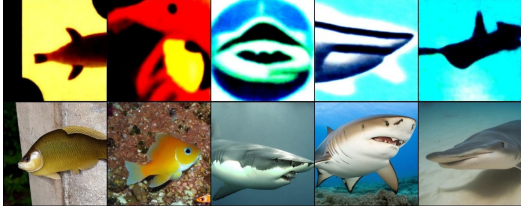


Figure 7. Universal Guidance (top) vs Longtail Guidance (bottom). Universal Guidance, when driven by model-based longtail signals, successfully raises those signals but it does so by generating data that is no longer in-distribution. It is also much more expensive.

the predictive model performing guidance does not need to be trained on intermediate diffusion states:  $D(P(x_t))$  is closer in distribution to real training data than is  $x_t$ .

LTG requires no training for either the diffusion or the production model. Each can be used off-the-shelf. It’s primary limitation is that the gradient  $d\hat{x}_t^0/d\hat{z}_t^0$  calculated by decoding is expensive (see Supplement A.6).

## 4. Experiments

In Section 4.1, we compare predictive model generalization improvements when training data is augmented with synthetic data generated by Longtail Guidance, when training data is augmented with existing synthetic data generation approaches, and when training data is augmented with traditional data augmentations approaches. In Section 4.2, we reduce synthetic data generated with Longtail Guidance to a set of text descriptions that describe attributes of a predictive model’s longtail. We demonstrate that these descriptions are meaningful by showing that they produce higher-value synthetic data than manually prompt-tuned diffusion. In Supplement A.1, we additionally demonstrate that LTG improves the ImageNet-LT generalization performance of SOTA ViT models that compensate for class-imbalance. In Section 4.3, we examine why Longtail Guidance outperforms existing synthetic data generation approaches.

### 4.1. LTG Improves Predictive Model Generalization

We compare Longtail Guidance with three measures (Epistemic, Entropy, Energy) to the recent Guided Imagination Framework (GIF) (Zhang et al., 2023b) and Dream the Impossible (Dream-ID) (Du et al., 2024) synthetic data generation approaches. For baselines, we compare to prompt-tuned Stable Diffusion 1.4 (SD), prompt-tuned DALL-E2, and masked autoencoder (MAE) data generation (He et al., 2022). We also compare to data augmentation baselines: Cutout (DeVries, 2017), GridMask (Chen et al., 2020), RandAugment (Cubuk et al., 2020), AutoAugment (Cubuk et al., 2019), CutMix (Yun et al., 2019), AugMix (Hendrycks et al., 2019) and adversarial robustness approaches DeepAugment (Hendrycks et al., 2021), and MEMO (Zhang et al., 2022a).

Finally, we report CLIP zero-shot and distillation performance (Radford et al., 2021).

We evaluate on seven natural image datasets spanning fine-grained, coarse-grained, and mixed coarse/fine classification tasks. Datasets include ImageNet, ImageNet-V2, ImageNet-A, Stanford Cars (Krause et al., 2013), Oxford Flowers (Nilsback & Zisserman, 2008), Oxford Pets (Parkhi et al., 2012), and Caltech101 (Fei-Fei et al., 2004). We reproduce baseline predictive models (Original) that are not exposed to synthetic data, with comparable performance (within 1%) of the baselines used in (Du et al., 2024; Zhang et al., 2023b).<sup>1</sup> We iteratively perform additional fine-tuning with synthetic training data that is equal in quantity across all conditions, use the same augmentations (random rotation, reflection, and center cropping), and report generalization performance as top-1 accuracy. Results are averaged over three runs. Additional experiment details are in Supplement A.2 and dataset details are in Supplement A.4. We fix hyperparameters (LTG weight, number of Epistemic Heads) across all datasets according to Supplement A.9.

In Table 1, we compare to baselines under the Dataset Expansion task as defined in GIF (Zhang et al., 2023b). For parity, we fine-tune ResNet-50 models for 100 epochs and generate synthetic data equivalent to  $20\times$  the original dataset size for Caltech, Cars and Flowers, and  $30\times$  the original dataset size for Pets. GIF generates all synthetic data at once whereas we evenly distribute data generation throughout training epochs to better capture evolving model-based longtail challenges, see Supplement A.2 for details. In each expansion, synthetic examples per class are equal in quantity to the original number of real examples.

In Table 2, we compare to baselines under the in-distribution synthetic data generation task as defined in Dream the Impossible (Du et al., 2024) and discussed in Supplement A.2. For parity, we train ResNet-34 models for 100 epochs and generate 1k synthetic data per class. Models are trained on ImageNet-100 and evaluated on ImageNet-100, ImageNet-A, and ImageNet-V2 subsets defined in Supplement A.4.

In each benchmark, Longtail Guidance provides substantial improvements over existing synthetic data generation methods and data augmentation baselines. In particular, it provides an average 5.6 points of additional top-1 accuracy compared to GIF or Dream-ID, and an average 15.0 points of additional top-1 accuracy compared to text-prompted Stable Diffusion. Aggregate improvements from the Epistemic Head over alternative model-based longtail signals (energy, entropy) are mild but significant and come at negligible inference or training time cost as described in Supplement A.6. In Supplement A.5, we show that predictive model general-

<sup>1</sup>Baseline model checkpoints were not available so we reproduce them using the reported architecture and training recipe.

ization can be further improved by engaging in more cycles of fine-tuning and synthetic data generation.

Table 1. Top-1 Accuracy on coarse-grained (Caltech) and fine-grained (Pets, Cars, Flowers) natural image datasets under the Dataset Expansion task as defined in (Zhang et al., 2023b).

Dataset	Caltech	Cars	Flowers	Pets	Avg
Original	26.3	19.8	74.1	6.8	31.8
CLIP	82.1	55.8	71.2	85.4	72.3
CLIP Distill	33.2	18.9	75.1	11.1	34.6
<b>Expanded</b>					
Cutout	51.5	25.8	77.8	38.7	48.5
GridMask	51.6	28.4	80.7	37.6	49.6
RandAugment	57.8	43.2	83.8	48.0	58.2
MAE	50.6	25.9	76.3	39.9	48.2
DALL-E2	61.3	48.3	84.1	61.7	63.8
SD	51.1	51.7	78.8	57.9	59.9
GIF-MAE	58.4	44.5	84.4	52.4	59.9
GIF-DALLE	63.0	53.1	88.2	66.4	67.7
GIF-SD	65.1	75.7	88.3	73.4	75.6
LTG (Energy)	70.4	<b>85.3</b>	90.3	80.0	81.5
LTG (Entropy)	70.6	84.6	89.9	81.6	81.7
LTG (Epistemic)	<b>71.5</b>	85.1	<b>90.9</b>	<b>82.0</b>	<b>82.4</b>

Table 2. Top-1 Accuracy on the in-distribution synthetic data generation task for ImageNet variants as defined in (Du et al., 2024)

Methods	ImageNet	ImageNet-A	ImageNet-v2	Avg
Original	87.28	8.69	77.80	57.92
RandAugment	88.10	11.39	78.90	59.46
CutMix	87.98	9.67	79.70	59.12
AutoAugment	88.00	10.85	79.70	59.52
AugMix	87.74	10.96	79.20	59.30
DeepAugment	86.86	10.79	78.30	58.65
MEMO	88.00	10.85	78.60	59.15
SD	87.74	11.18	79.20	59.37
DREAM-ID	88.46	12.13	80.40	60.33
LTG (Energy)	90.00	20.20	81.05	63.75
LTG (Entropy)	90.04	<b>22.70</b>	80.66	64.47
LTG (Epistemic)	<b>90.30</b>	22.09	<b>81.54</b>	<b>64.64</b>

## 4.2. LTG Produces Meaningful Longtail Data

We examine synthetic data generated by LTG to determine whether they exhibit meaningful variation from baseline synthetic data generated by prompt-tuned diffusion. This is a difficult and fundamentally qualitative task to manually perform at scale. To make it quantitative, we ask: do text descriptions of LTG-generated data lead to predictive model generalization improvements when they are used to generate additional synthetic data (without LTG)?

Starting with the strongest baseline model  $f_\phi$  trained on Flowers (Original from Table 1), we ask a VLM (Liu et al., 2024) to caption real training instances  $x_{\text{real}}$  and also synthetic data  $x_{\text{ltg}}$  generated by LTG as guided by  $f_\phi^{\text{lt}}$ . For each synthetic instance,  $N$  novel keywords are found by computing the token embeddings that are furthest in cosine

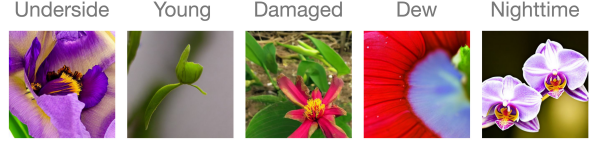


Figure 8. Longtail keywords from LTG-generated Flowers data.

similarity from all real data token embeddings. An LLM (OpenAI, 2023) is then provided with a set of (caption, novel keyword) pairs for each class and asked to summarize them into  $P$  refined prompts. We call this Longtail Introspection.

Refined prompts are used to generate additional synthetic data  $x_{\text{inspect}}$  by diffusion (without LTG). We train  $f_\phi$  on synthetic data generated by Longtail Introspection and compare it to synthetic data generated by manual prompt tuning (40 unique prompts per class, as in (Zhang et al., 2023b); details in Supplement A.3). Table 3 shows that Longtail Introspection significantly outperforms manually prompt-tuned diffusion (defined in Supplement A.2), quantitatively supporting that data generated by LTG exhibit meaningful variation. Figure 8 shows example longtail keywords.

Table 3. Synthetic data generated by prompts based on VLM descriptions of LTG data outperform synthetic data generated by manually prompt-tuned diffusion, quantitatively suggesting that data generated by LTG exhibit meaningful and challenging variation from the perspective of predictive model  $f_\phi$ .

Condition	Accuracy
No Synthetic Data	74.1
Manual Prompt Tuning	78.8
Longtail Introspection	<b>84.3</b>

## 4.3. Discussion

Longtail Guidance significantly outperforms leading synthetic data generation baselines including GIF and Dream-ID even though it requires no prompt tuning. To explain this, we note that GIF and Dream-ID reason in latent CLIP space to create new embedding vectors with which to prompt a diffusion model. For each real data instance, GIF creates  $K$  additional synthetic instances by jointly optimizing  $K$  embedding vectors (initialized by CLIP image encoding) such that they are difficult for CLIP zero-shot classification (high entropy), remain close to the target class (high log prob of target class), and diverse (high KL divergence to a mean embedding). In Dream-ID, a separate model is trained to predict class embedding vectors from (real data, CLIP-based class text embedding vector) pairs. From this, a manifold in CLIP space can be sampled along class boundaries to generate new diffusion conditioning vectors.

We posit that synthesizing data that is difficult or rare for a foundation model, like CLIP, is different from synthesizing data that is difficult or rare for a specific, deployed predictive



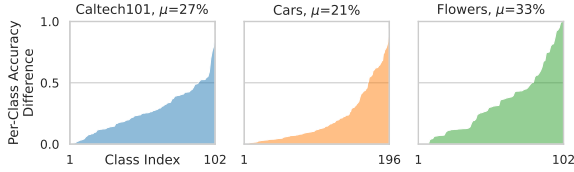


Figure 9. Reasoning in latent CLIP space for synthetic data generation does not account for differences in what is difficult for CLIP versus what is difficult for a production model. We plot (sorted) absolute difference in per-class accuracy between a CLIP zero-shot classifier and a well-trained production model. Even when aggregate performance is similar, as in Flowers (74.0% vs 71.2% top-1 accuracy), average per-class difference is high (33%).

model. Figure 9 quantifies this by showing that, even when CLIP zero-shot performance and a production model have similar aggregate performance 74.1% vs 71.2%, the classes (and data instances) that are difficult for CLIP are different from the classes that are difficult for the production model—with average per-class accuracy differences of 34%!

In both GIF and Dream-ID, reasoning is only conditioned on training data and restricted to CLIP embedding space. In Longtail Guidance, we instead condition on longtail signals coming directly from the predictive model we wish to improve. We know that these signals identify rare or disproportionately hard examples (Figure 5) and that synthetic data generated by LTG reliably have lower probability of correct classification, lower accuracy, and higher longtail signals (Figure 2) under the predictive model. This is most strikingly demonstrated in the more than 80% generalization improvement over Dream-ID on the naturally challenging examples of ImageNet-A.

## 5. Related Work

Diffusion has seen wide success, particularly in image generation, where it outperforms GANs in image quality and diversity without suffering from unstable training or mode collapse (Dhariwal & Nichol, 2021). Recent work has seen progress in handling large data dimensions with latent spaces (Chen et al., 2025; Podell et al., 2023; Rombach et al., 2022) or hourglass networks (Crowson et al., 2024), improved sampling (Lu et al., 2022; Karras et al., 2022; Ho et al., 2020; Song et al., 2020a), additional data domains (Ran et al., 2024; Pronovost et al., 2023; Zhong et al., 2023), and personalization (Ruiz et al., 2023; Kumari et al., 2023). Much work has also been done on new forms of guidance (Wallace et al., 2023b; Yu et al., 2023a; Wallace et al., 2023a; Zhang et al., 2023a) beyond just classifier guidance and classifier-free guidance (Dhariwal & Nichol, 2021; Ho & Salimans, 2022). Universal Guidance (Bansal et al., 2023) is most relevant, and is discussed in Section 3.

Synthetic training data from generative models has been

considered since GANs (Li et al., 2022b), but has started to come of age with diffusion (Azizi et al., 2023; Zhou et al., 2023), particularly for high-resolution datasets where fidelity matters. GIF (Zhang et al., 2023b) and Dream-ID (Du et al., 2024), discussed in Section 4.3, are most relevant.

Model signals have been used for out-of-distribution or adversarial detection (Huang et al., 2021; Hsu et al., 2020; Cohen et al., 2020), particularly model uncertainty (Van Amersfoort et al., 2020) or feature density (Lee et al., 2018). Epistemic uncertainty has been developed in (expensive) Bayesian (Gal & Ghahramani, 2016) or model ensemble contexts (Liu et al., 2019a; Depeweg et al., 2018; Wilson & Izmailov, 2020; Lakshminarayanan et al., 2017), though, to our knowledge, not explicitly in a single, differentiable forward pass as we have done in Section 2.1. Work on longtail robustness has primarily focused on addressing a-priori known class imbalance. Datasets include ImageNet-LT, Places-LT, (Liu et al., 2019b) and iNaturalist (Van Horn et al., 2018). Mitigations include pretraining (He et al., 2022; Bao et al., 2021), distillation (Xiang et al., 2020), reweighted losses (Xu et al., 2023; Ross & Dollár, 2017), or selective (real) data mining (Jiang et al., 2022).

## Conclusion

We developed model-based longtail signals that do not impact model weights or performance and are leveraged by Longtail Guidance, a synthetic data generation approach that explicitly conditions on an existing predictive model to generate examples that are rare or hard from that model’s perspective. We show that training on LTG-generated data provides stronger generalization improvements than synthetic data generation and data augmentation baselines over eight datasets. We further demonstrate that longtail synthetic data generations can be rendered into meaningful text descriptions that can aid future (real or synthetic) data collection priorities.

Predictive models are being deployed more than ever before. Increasingly, they will encounter longtail scenarios that human operators cannot predict in advance. Foundation models can be used to mitigate some risk, but we cannot shoehorn the entirety of Internet-scale knowledge into every deployed model due to capacity and compute constraints. By letting an existing predictive model *speak for itself*, we can expend offline compute to generatively mine high-value synthetic training data. Further reducing these synthetic examples to human- and machine-readable text suggests a future where we can move away from slow, reactive longtail mitigation towards fast, proactive longtail discovery.



## References

- Anthropic. Introducing the next generation of claude, 2024. URL <https://www.anthropic.com/news/claude-3-family>. Accessed: 2025-01-03.
- Azizi, S., Kornblith, S., Saharia, C., Norouzi, M., and Fleet, D. J. Synthetic data from diffusion models improves imagenet classification. *arXiv preprint arXiv:2304.08466*, 2023.
- Bansal, A., Chu, H.-M., Schwarzschild, A., Sengupta, S., Goldblum, M., Geiping, J., and Goldstein, T. Universal guidance for diffusion models. In *Proceedings of the IEEE/CVF Conference on Computer Vision and Pattern Recognition*, pp. 843–852, 2023.
- Bansal, H. and Grover, A. Leaving reality to imagination: Robust classification via generated datasets. *arXiv preprint arXiv:2302.02503*, 2023.
- Bao, H., Dong, L., Piao, S., and Wei, F. Beit: Bert pre-training of image transformers. *arXiv preprint arXiv:2106.08254*, 2021.
- Brown, T., Mann, B., Ryder, N., Subbiah, M., Kaplan, J. D., Dhariwal, P., Neelakantan, A., Shyam, P., Sastry, G., Askell, A., et al. Language models are few-shot learners. *Advances in neural information processing systems*, 33: 1877–1901, 2020.
- Cai, J., Wang, Y., and Hwang, J.-N. Ace: Ally complementary experts for solving long-tailed recognition in one-shot. In *Proceedings of the IEEE/CVF international conference on computer vision*, pp. 112–121, 2021.
- Cao, K., Wei, C., Gaidon, A., Arechiga, N., and Ma, T. Learning imbalanced datasets with label-distribution-aware margin loss. *Advances in neural information processing systems*, 32, 2019.
- Chen, J., Ge, C., Xie, E., Wu, Y., Yao, L., Ren, X., Wang, Z., Luo, P., Lu, H., and Li, Z. Pixart- $\sigma$ : Weak-to-strong training of diffusion transformer for 4k text-to-image generation. In *European Conference on Computer Vision*, pp. 74–91. Springer, 2025.
- Chen, P., Liu, S., Zhao, H., Wang, X., and Jia, J. Gridmask data augmentation. *arXiv preprint arXiv:2001.04086*, 2020.
- Cohen, G., Sapiro, G., and Giryes, R. Detecting adversarial samples using influence functions and nearest neighbors. In *Proceedings of the IEEE/CVF conference on computer vision and pattern recognition*, pp. 14453–14462, 2020.
- Crowson, K., Baumann, S. A., Birch, A., Abraham, T. M., Kaplan, D. Z., and Shippole, E. Scalable high-resolution pixel-space image synthesis with hourglass diffusion transformers. In *Forty-first International Conference on Machine Learning*, 2024.
- Cubuk, E. D., Zoph, B., Mane, D., Vasudevan, V., and Le, Q. V. Autoaugment: Learning augmentation strategies from data. In *Proceedings of the IEEE/CVF conference on computer vision and pattern recognition*, pp. 113–123, 2019.
- Cubuk, E. D., Zoph, B., Shlens, J., and Le, Q. V. Randaugment: Practical automated data augmentation with a reduced search space. In *Proceedings of the IEEE/CVF conference on computer vision and pattern recognition workshops*, pp. 702–703, 2020.
- Cui, J., Zhong, Z., Liu, S., Yu, B., and Jia, J. Parametric contrastive learning. In *Proceedings of the IEEE/CVF international conference on computer vision*, pp. 715–724, 2021.
- Cui, Y., Jia, M., Lin, T.-Y., Song, Y., and Belongie, S. Class-balanced loss based on effective number of samples. In *Proceedings of the IEEE/CVF conference on computer vision and pattern recognition*, pp. 9268–9277, 2019.
- Depeweg, S., Hernandez-Lobato, J.-M., Doshi-Velez, F., and Udluft, S. Decomposition of uncertainty in bayesian deep learning for efficient and risk-sensitive learning. In *International conference on machine learning*, pp. 1184–1193. PMLR, 2018.
- Devlin, J. Bert: Pre-training of deep bidirectional transformers for language understanding. *arXiv preprint arXiv:1810.04805*, 2018.
- DeVries, T. Improved regularization of convolutional neural networks with cutout. *arXiv preprint arXiv:1708.04552*, 2017.
- Dhariwal, P. and Nichol, A. Diffusion models beat gans on image synthesis. *Advances in neural information processing systems*, 34:8780–8794, 2021.
- Dosovitskiy, A. An image is worth 16x16 words: Transformers for image recognition at scale. *arXiv preprint arXiv:2010.11929*, 2020.
- Du, X., Sun, Y., Zhu, J., and Li, Y. Dream the impossible: Outlier imagination with diffusion models. *Advances in Neural Information Processing Systems*, 36, 2024.
- Fei-Fei, L., Fergus, R., and Perona, P. Learning generative visual models from few training examples: An incremental bayesian approach tested on 101 object categories. In *2004 conference on computer vision and pattern recognition workshop*, pp. 178–178. IEEE, 2004.

- Gal, Y. and Ghahramani, Z. Dropout as a bayesian approximation: Representing model uncertainty in deep learning. In *international conference on machine learning*, pp. 1050–1059. PMLR, 2016.
- Gou, J., Yu, B., Maybank, S. J., and Tao, D. Knowledge distillation: A survey. *International Journal of Computer Vision*, 129(6):1789–1819, 2021.
- Gowal, S., Rebuffi, S.-A., Wiles, O., Stimberg, F., Calian, D. A., and Mann, T. A. Improving robustness using generated data. *Advances in Neural Information Processing Systems*, 34:4218–4233, 2021.
- Guzman-Rivera, A., Batra, D., and Kohli, P. Multiple choice learning: Learning to produce multiple structured outputs. *Advances in neural information processing systems*, 25, 2012.
- He, K., Chen, X., Xie, S., Li, Y., Dollár, P., and Girshick, R. Masked autoencoders are scalable vision learners. In *Proceedings of the IEEE/CVF conference on computer vision and pattern recognition*, pp. 16000–16009, 2022.
- Hendrycks, D., Mu, N., Cubuk, E. D., Zoph, B., Gilmer, J., and Lakshminarayanan, B. Augmix: A simple data processing method to improve robustness and uncertainty. *arXiv preprint arXiv:1912.02781*, 2019.
- Hendrycks, D., Basart, S., Mu, N., Kadavath, S., Wang, F., Dorundo, E., Desai, R., Zhu, T., Parajuli, S., Guo, M., et al. The many faces of robustness: A critical analysis of out-of-distribution generalization. In *Proceedings of the IEEE/CVF international conference on computer vision*, pp. 8340–8349, 2021.
- Heusel, M., Ramsauer, H., Unterthiner, T., Nessler, B., and Hochreiter, S. Gans trained by a two time-scale update rule converge to a local nash equilibrium. *Advances in neural information processing systems*, 30, 2017.
- Ho, J. and Salimans, T. Classifier-free diffusion guidance. *arXiv preprint arXiv:2207.12598*, 2022.
- Ho, J., Jain, A., and Abbeel, P. Denoising diffusion probabilistic models. *Advances in neural information processing systems*, 33:6840–6851, 2020.
- Hong, Y., Zhang, J., Sun, Z., and Yan, K. Safa: Sample-adaptive feature augmentation for long-tailed image classification. In *European Conference on Computer Vision*, pp. 587–603. Springer, 2022.
- Hsu, Y.-C., Shen, Y., Jin, H., and Kira, Z. Generalized odin: Detecting out-of-distribution image without learning from out-of-distribution data. In *Proceedings of the IEEE/CVF conference on computer vision and pattern recognition*, pp. 10951–10960, 2020.
- Hu, E. J., Shen, Y., Wallis, P., Allen-Zhu, Z., Li, Y., Wang, S., Wang, L., and Chen, W. Lora: Low-rank adaptation of large language models. *arXiv preprint arXiv:2106.09685*, 2021.
- Huang, R., Geng, A., and Li, Y. On the importance of gradients for detecting distributional shifts in the wild. *Advances in Neural Information Processing Systems*, 34: 677–689, 2021.
- Jang, E., Gu, S., and Poole, B. Categorical reparameterization with gumbel-softmax. *arXiv preprint arXiv:1611.01144*, 2016.
- Jiang, C., Cornman, A., Park, C., Sapp, B., Zhou, Y., Anguelov, D., et al. Motiondiffuser: Controllable multi-agent motion prediction using diffusion. In *Proceedings of the IEEE/CVF Conference on Computer Vision and Pattern Recognition*, pp. 9644–9653, 2023.
- Jiang, C. M., Najibi, M., Qi, C. R., Zhou, Y., and Anguelov, D. Improving the intra-class long-tail in 3d detection via rare example mining. In *European Conference on Computer Vision*, pp. 158–175. Springer, 2022.
- Kang, B., Xie, S., Rohrbach, M., Yan, Z., Gordo, A., Feng, J., and Kalantidis, Y. Decoupling representation and classifier for long-tailed recognition. *arXiv preprint arXiv:1910.09217*, 2019.
- Kaplan, J., McCandlish, S., Henighan, T., Brown, T. B., Chess, B., Child, R., Gray, S., Radford, A., Wu, J., and Amodei, D. Scaling laws for neural language models. *arXiv preprint arXiv:2001.08361*, 2020.
- Karras, T., Aittala, M., Aila, T., and Laine, S. Elucidating the design space of diffusion-based generative models. *Advances in neural information processing systems*, 35: 26565–26577, 2022.
- Krause, J., Deng, J., Stark, M., and Fei-Fei, L. Collecting a large-scale dataset of fine-grained cars. 2013.
- Kumari, N., Zhang, B., Zhang, R., Shechtman, E., and Zhu, J.-Y. Multi-concept customization of text-to-image diffusion. In *Proceedings of the IEEE/CVF Conference on Computer Vision and Pattern Recognition*, pp. 1931–1941, 2023.
- Lakshminarayanan, B., Pritzel, A., and Blundell, C. Simple and scalable predictive uncertainty estimation using deep ensembles. *Advances in neural information processing systems*, 30, 2017.
- Lee, K., Lee, K., Lee, H., and Shin, J. A simple unified framework for detecting out-of-distribution samples and adversarial attacks. *Advances in neural information processing systems*, 31, 2018.

- Li, B., Han, Z., Li, H., Fu, H., and Zhang, C. Trustworthy long-tailed classification. In *Proceedings of the IEEE/CVF Conference on Computer Vision and Pattern Recognition*, pp. 6970–6979, 2022a.
- Li, D., Ling, H., Kim, S. W., Kreis, K., Fidler, S., and Torralba, A. Bigdatasetgan: Synthesizing imagenet with pixel-wise annotations. In *Proceedings of the IEEE/CVF Conference on Computer Vision and Pattern Recognition*, pp. 21330–21340, 2022b.
- Li, J., Tan, Z., Wan, J., Lei, Z., and Guo, G. Nested collaborative learning for long-tailed visual recognition. In *Proceedings of the IEEE/CVF Conference on Computer Vision and Pattern Recognition*, pp. 6949–6958, 2022c.
- Li, M., Cheung, Y.-m., and Lu, Y. Long-tailed visual recognition via gaussian clouded logit adjustment. In *Proceedings of the IEEE/CVF Conference on Computer Vision and Pattern Recognition*, pp. 6929–6938, 2022d.
- Li, T., Cao, P., Yuan, Y., Fan, L., Yang, Y., Feris, R. S., Indyk, P., and Katabi, D. Targeted supervised contrastive learning for long-tailed recognition. In *Proceedings of the IEEE/CVF conference on computer vision and pattern recognition*, pp. 6918–6928, 2022e.
- Liu, H., Li, C., Li, Y., Li, B., Zhang, Y., Shen, S., and Lee, Y. J. Llava-next: Improved reasoning, ocr, and world knowledge, January 2024. URL <https://llava-vl.github.io/blog/2024-01-30-llava-next/>.
- Liu, J., Paisley, J., Kioumourtzoglou, M.-A., and Coull, B. Accurate uncertainty estimation and decomposition in ensemble learning. *Advances in neural information processing systems*, 32, 2019a.
- Liu, W., Wang, X., Owens, J., and Li, Y. Energy-based out-of-distribution detection. *Advances in neural information processing systems*, 33:21464–21475, 2020.
- Liu, Z., Miao, Z., Zhan, X., Wang, J., Gong, B., and Yu, S. X. Large-scale long-tailed recognition in an open world. In *Proceedings of the IEEE/CVF conference on computer vision and pattern recognition*, pp. 2537–2546, 2019b.
- Lu, C., Zhou, Y., Bao, F., Chen, J., Li, C., and Zhu, J. Dpm-solver++: Fast solver for guided sampling of diffusion probabilistic models. *arXiv preprint arXiv:2211.01095*, 2022.
- Maddox, W. J., Izmailov, P., Garipov, T., Vetrov, D. P., and Wilson, A. G. A simple baseline for bayesian uncertainty in deep learning. *Advances in neural information processing systems*, 32, 2019.
- Minsky, M. *The Emotion Machine: Commonsense Thinking, Artificial Intelligence, and the Future of the Human Mind*. Simon and Schuster, 2006. ISBN 9780743276641.
- Nilsback, M.-E. and Zisserman, A. Automated flower classification over a large number of classes. In *2008 Sixth Indian conference on computer vision, graphics & image processing*, pp. 722–729. IEEE, 2008.
- OpenAI. Gpt-4 technical report. Technical report, OpenAI, 2023. URL <https://openai.com/research/gpt-4>.
- Parkhi, O. M., Vedaldi, A., Zisserman, A., and Jawahar, C. Cats and dogs. In *2012 IEEE conference on computer vision and pattern recognition*, pp. 3498–3505. IEEE, 2012.
- Podell, D., English, Z., Lacey, K., Blattmann, A., Dockhorn, T., Müller, J., Penna, J., and Rombach, R. Sdxl: Improving latent diffusion models for high-resolution image synthesis. *arXiv preprint arXiv:2307.01952*, 2023.
- Pronovost, E., Ganesina, M. R., Hendy, N., Wang, Z., Morales, A., Wang, K., and Roy, N. Scenario diffusion: Controllable driving scenario generation with diffusion. *Advances in Neural Information Processing Systems*, 36: 68873–68894, 2023.
- Radford, A., Kim, J. W., Hallacy, C., Ramesh, A., Goh, G., Agarwal, S., Sastry, G., Askell, A., Mishkin, P., Clark, J., et al. Learning transferable visual models from natural language supervision. In *International conference on machine learning*, pp. 8748–8763. PMLR, 2021.
- Ran, H., Guizilini, V., and Wang, Y. Towards realistic scene generation with lidar diffusion models. In *Proceedings of the IEEE/CVF Conference on Computer Vision and Pattern Recognition*, pp. 14738–14748, 2024.
- Rombach, R., Blattmann, A., Lorenz, D., Esser, P., and Ommer, B. High-resolution image synthesis with latent diffusion models. In *Proceedings of the IEEE/CVF conference on computer vision and pattern recognition*, pp. 10684–10695, 2022.
- Ross, T.-Y. and Dollár, G. Focal loss for dense object detection. In *proceedings of the IEEE conference on computer vision and pattern recognition*, pp. 2980–2988, 2017.
- Ruiz, N., Li, Y., Jampani, V., Pritch, Y., Rubinstein, M., and Aberman, K. Dreambooth: Fine tuning text-to-image diffusion models for subject-driven generation. In *Proceedings of the IEEE/CVF conference on computer vision and pattern recognition*, pp. 22500–22510, 2023.



- Song, J., Meng, C., and Ermon, S. Denoising diffusion implicit models. *arXiv preprint arXiv:2010.02502*, 2020a.
- Song, Y., Sohl-Dickstein, J., Kingma, D. P., Kumar, A., Ermon, S., and Poole, B. Score-based generative modeling through stochastic differential equations. *arXiv preprint arXiv:2011.13456*, 2020b.
- Tang, K., Huang, J., and Zhang, H. Long-tailed classification by keeping the good and removing the bad momentum causal effect. *Advances in neural information processing systems*, 33:1513–1524, 2020.
- Touvron, H., Cord, M., and Jégou, H. Deit iii: Revenge of the vit. In *European conference on computer vision*, pp. 516–533. Springer, 2022.
- Tran, L., Veeling, B. S., Roth, K., Swiatkowski, J., Dillon, J. V., Snoek, J., Mandt, S., Salimans, T., Nowozin, S., and Jenatton, R. Hydra: Preserving ensemble diversity for model distillation. *arXiv preprint arXiv:2001.04694*, 2020.
- Van Amersfoort, J., Smith, L., Teh, Y. W., and Gal, Y. Uncertainty estimation using a single deep deterministic neural network. In *International conference on machine learning*, pp. 9690–9700. PMLR, 2020.
- Van Horn, G., Mac Aodha, O., Song, Y., Cui, Y., Sun, C., Shepard, A., Adam, H., Perona, P., and Belongie, S. The inaturalist species classification and detection dataset. In *Proceedings of the IEEE conference on computer vision and pattern recognition*, pp. 8769–8778, 2018.
- Wallace, B., Gokul, A., Ermon, S., and Naik, N. End-to-end diffusion latent optimization improves classifier guidance. In *Proceedings of the IEEE/CVF International Conference on Computer Vision*, pp. 7280–7290, 2023a.
- Wallace, B., Gokul, A., and Naik, N. Edict: Exact diffusion inversion via coupled transformations. In *Proceedings of the IEEE/CVF Conference on Computer Vision and Pattern Recognition*, pp. 22532–22541, 2023b.
- Wang, H., Fu, S., He, X., Fang, H., Liu, Z., and Hu, H. Towards calibrated hyper-sphere representation via distribution overlap coefficient for long-tailed learning. In *European Conference on Computer Vision*, pp. 179–196. Springer, 2022.
- Wang, X., Lian, L., Miao, Z., Liu, Z., and Yu, S. X. Long-tailed recognition by routing diverse distribution-aware experts. *arXiv preprint arXiv:2010.01809*, 2020.
- Wei, J., Wang, X., Schuurmans, D., Bosma, M., Xia, F., Chi, E., Le, Q. V., Zhou, D., et al. Chain-of-thought prompting elicits reasoning in large language models. *Advances in neural information processing systems*, 35:24824–24837, 2022.
- Wilson, A. G. and Izmailov, P. Bayesian deep learning and a probabilistic perspective of generalization. *Advances in neural information processing systems*, 33:4697–4708, 2020.
- Xiang, L., Ding, G., and Han, J. Learning from multiple experts: Self-paced knowledge distillation for long-tailed classification. In *Computer Vision–ECCV 2020: 16th European Conference, Glasgow, UK, August 23–28, 2020, Proceedings, Part V 16*, pp. 247–263. Springer, 2020.
- Xu, Y., Li, Y.-L., Li, J., and Lu, C. Constructing balance from imbalance for long-tailed image recognition. In *European Conference on Computer Vision*, pp. 38–56. Springer, 2022.
- Xu, Z., Liu, R., Yang, S., Chai, Z., and Yuan, C. Learning imbalanced data with vision transformers. In *Proceedings of the IEEE/CVF conference on computer vision and pattern recognition*, pp. 15793–15803, 2023.
- Yao, S., Yu, D., Zhao, J., Shafran, I., Griffiths, T., Cao, Y., and Narasimhan, K. Tree of thoughts: Deliberate problem solving with large language models. *Advances in Neural Information Processing Systems*, 36, 2024.
- Yu, F., Chen, H., Wang, X., Xian, W., Chen, Y., Liu, F., Madhavan, V., and Darrell, T. Bdd100k: A diverse driving dataset for heterogeneous multitask learning. In *Proceedings of the IEEE/CVF conference on computer vision and pattern recognition*, pp. 2636–2645, 2020.
- Yu, J., Wang, Y., Zhao, C., Ghanem, B., and Zhang, J. Freedom: Training-free energy-guided conditional diffusion model. In *Proceedings of the IEEE/CVF International Conference on Computer Vision*, pp. 23174–23184, 2023a.
- Yu, R., Liu, S., and Wang, X. Dataset distillation: A comprehensive review. *IEEE Transactions on Pattern Analysis and Machine Intelligence*, 2023b.
- Yun, S., Han, D., Oh, S. J., Chun, S., Choe, J., and Yoo, Y. Cutmix: Regularization strategy to train strong classifiers with localizable features. In *Proceedings of the IEEE/CVF international conference on computer vision*, pp. 6023–6032, 2019.
- Zhang, L., Rao, A., and Agrawala, M. Adding conditional control to text-to-image diffusion models. In *Proceedings of the IEEE/CVF International Conference on Computer Vision*, pp. 3836–3847, 2023a.
- Zhang, M., Levine, S., and Finn, C. Memo: Test time robustness via adaptation and augmentation. *Advances in neural information processing systems*, 35:38629–38642, 2022a.

- Zhang, S., Li, Z., Yan, S., He, X., and Sun, J. Distribution alignment: A unified framework for long-tail visual recognition. In *Proceedings of the IEEE/CVF conference on computer vision and pattern recognition*, pp. 2361–2370, 2021.
- Zhang, Y., Hooi, B., Hong, L., and Feng, J. Self-supervised aggregation of diverse experts for test-agnostic long-tailed recognition. *Advances in Neural Information Processing Systems*, 35:34077–34090, 2022b.
- Zhang, Y., Zhou, D., Hooi, B., Wang, K., and Feng, J. Expanding small-scale datasets with guided imagination. *Advances in neural information processing systems*, 36: 76558–76618, 2023b.
- Zhong, Z., Cui, J., Liu, S., and Jia, J. Improving calibration for long-tailed recognition. In *Proceedings of the IEEE/CVF conference on computer vision and pattern recognition*, pp. 16489–16498, 2021.
- Zhong, Z., Rempe, D., Chen, Y., Ivanovic, B., Cao, Y., Xu, D., Pavone, M., and Ray, B. Language-guided traffic simulation via scene-level diffusion. In *Conference on Robot Learning*, pp. 144–177. PMLR, 2023.
- Zhou, Y., Sahak, H., and Ba, J. Training on thin air: Improve image classification with generated data. *arXiv preprint arXiv:2305.15316*, 2023.
- Zhu, J., Wang, Z., Chen, J., Chen, Y.-P. P., and Jiang, Y.-G. Balanced contrastive learning for long-tailed visual recognition. In *Proceedings of the IEEE/CVF Conference on Computer Vision and Pattern Recognition*, pp. 6908–6917, 2022.

## A. Appendix

### A.1. LTG Improves Longtail Performance

In Table 4, we train SOTA ViT-based models (LiVT) from scratch on ImageNet-LT according to the longtail-compensation approach of (Xu et al., 2023). In summary, training includes MAE pretraining followed by 100 epochs of BCE loss with a logit adjustment to account for class imbalance. Initial LiVT training is on real data only and uses many data augmentations including RandAugment, Mixup, and CutMix. Our baseline predictive model, LiVT (Reproduced), nearly matches the generalization performance (top-1 accuracy) of what is reported in (Xu et al., 2023) (LiVT (Reproduced): 60.6 vs LiVT (Reported): 60.9). We then fine-tune LiVT on 24000 additional synthetic data evenly distributed across all 1000 classes for 100 epochs with  $1e - 4$  learning rate. We use the same Stable Diffusion 1.4 baseline and sampling details as in the main paper (LiVT SD), and also compare Longtail Guidance with three types of model-based longtail signals (LiVT LTG {Energy, Entropy, Epistemic}). Overall generalization improvements on the balanced validation set are mild but significant (+1.3 top-1 accuracy). However, performance for longtail classes (Few) improves by four points for baseline diffusion (+10%) but a marked 10 points for Longtail Guidance (+24%)!

Synthetic data always improves Medium and Few performance, which are most impacted by a fixed number of data generations per class. This experiment demonstrates that Longtail Guidance works with multiple architectures (ResNet, ViT), multiple losses (CE, logit-adjusted BCE), and that it disproportionately improves longtail performance. It also demonstrates that LTG can be composed with finely-crafted training recipes to further improve predictive model generalization performance.

### A.2. Comparison to GIF and Dream-ID

In the main paper, Table 1, we compare to GIF, the Guided Imagination Framework (Zhang et al., 2023b). We use the same predictive model architecture (ResNet50 trained from scratch), generate the same quantity of synthetic data ( $30 \times$  dataset size for Pets,  $20 \times$  dataset size for Caltech101, Cars, and Flowers), the same diffusion model (Stable Diffusion v1.4), the same diffusion sampler (DDIM), and the same number of sampling iterates (50). We reproduce baseline models (not exposed to synthetic data or data augmentation conditions) to match the performance of GIF baselines (Original row in Table 1) to within 1% of the generalization performance reported in GIF. We then fine-tune for 100 epochs, generating synthetic data with Longtail Guidance according to the schedule in Table 5 (e.g. generate synthetic data in epoch 0, fine-tune until epoch 5, generate more synthetic data, fine-tune until epoch 10, ...). We experimentally found that synthetic data iteratively generated throughout fine-tuning outperformed synthetic data generated all at once and speculate that this is due to the model-based longtail evolving throughout training.

Synthetic data are distributed across classes according to their frequency in the original training data. Fine-tuning is with the Adam optimizer, cosine annealing learning rate schedule, and  $1e - 3$  learning rate. As in GIF, we train with random rotations ( $\pm 15^\circ$ ),  $224 \times 224$  crops, and horizontal flips.

In the main paper, Table 2, we compare to the in-distribution synthetic data generation task (Dream-ID) from Dream the Impossible (Du et al., 2024). As in Dream-ID, we start with ImageNet-pretrained ResNet-34 models and fine-tune for

Method	Many	Med.	Few	Acc
CE (Cui et al., 2019)	64.0	33.8	5.8	41.6
LDAM (Cao et al., 2019)	60.4	46.9	30.7	49.8
c-RT (Kang et al., 2019)	61.8	46.2	27.3	49.6
$\tau$ -Norm (Kang et al., 2019)	59.1	46.9	30.7	49.4
Causal (Tang et al., 2020)	62.7	48.8	31.6	51.8
Logit Adj. (Wang et al., 2020)	61.1	47.5	27.6	50.1
RIDE(4E) (Wang et al., 2020)	68.3	53.5	35.9	56.8
MiSLAS (Zhong et al., 2021)	62.9	50.7	34.3	52.7
DisAlign (Zhang et al., 2021)	61.3	52.2	31.4	52.9
ACE (Cai et al., 2021)	71.7	54.6	23.5	56.6
PaCo (Cui et al., 2021)	68.0	56.4	37.2	58.2
TADE (Zhang et al., 2022b)	66.5	57.0	43.5	58.8
TSC (Li et al., 2022e)	63.5	49.7	30.4	52.4
GCL (Li et al., 2022d)	63.0	52.7	37.1	54.5
TLC (Li et al., 2022a)	68.9	55.7	40.8	55.1
BCL (Zhu et al., 2022)	67.6	54.6	36.6	57.2
NCL (Li et al., 2022c)	67.3	55.4	39.0	57.7
SAFA (Hong et al., 2022)	63.8	49.9	33.4	53.1
DOC (Wang et al., 2022)	65.1	52.8	34.2	55.0
DLSA (Xu et al., 2022)	67.8	54.5	38.8	57.5
ViT (Dosovitskiy, 2020)	50.5	23.5	6.9	31.6
MAE (He et al., 2022)	<b>74.7</b>	48.2	19.4	54.5
DeiT (Touvron et al., 2022)	70.4	40.9	12.8	48.4
LiVT (Reproduced) (Xu et al., 2023)	72.7	56.6	40.4	60.6
LiVT SD	71.8	<b>58.1</b>	44.3	61.5
LiVT LTG (Energy)	70.5	57.9	<b>50.0</b>	61.7
LiVT LTG (Entropy)	70.9	57.9	49.8	61.8
LiVT LTG (Epistemic)	71.4	57.7	<b>50.0</b>	<b>61.9</b>

Table 4. Top-1 Accuracy on ImageNet-LT by dataset split (Many, Med, Few) and overall (Acc). The validation set is balanced between all 1000 classes but training is highly imbalanced: Few classes have 5 – 19 examples, Medium classes have 20 – 99 examples, Many classes have 100 – 1200 examples.



100 epochs with the same training details as above, except that we match the synthetic data quantity used in Dream-ID by generating a total of 1000 images per class, evenly distributed every 5 epochs (50 images per class per 5 epochs).

Different from GIF or Dream-ID is that we build synthetic data over the course of model fine-tuning, to better capture evolving model-based longtail challenges (whereas GIF, Dream-ID, and other synthetic data baselines generate all synthetic data at once since they are not model-conditioned). Also different is that LTG does not need prompt tuning to force synthetic data diversity. LTG text prompts are generic: “a photo of *Class*” whereas GIF prompts (and diffusion baselines) are, “a *Noun Adjective* of *Class*” where *Noun* is randomly sampled to be one of (“image”, “oil painting”, “cartoon image”, “sketch”, “pencil sketch”) and *Adjective* is randomly sampled to be one of (“”, “colorful”, “stylized”, “bright”, “sheared”, “solarized”, “posterized”, “high-contrast”), for a total of 40 unique prompts per class. In LTG, diversity is automatic based on the production model’s evolving longtail signals.

All experiments are performed on 8xH100.

Dataset	Total Expansion Ratio	Synthetic Data Generation Epochs
Pets	30×	0, 5, . . . , 45, 50; 52, 54, . . . , 96, 98
Caltech101, Cars, Flowers	20×	0, 5, . . . , 90, 95

Table 5. Synthetic Data Generation Schedule by Dataset

### A.3. Longtail Introspection

We construct refined prompts for each class by prompting LLaVA-1.6 7B (Liu et al., 2024) to generate a description for two sets of synthetic images: 100 generated by Longtail Guidance and 100 generated by baseline diffusion. VLM prompts are of the form: *This is an image of <Class>. Describe it in detail.* For each output VLM description, we compute per-token BERT embeddings (Devlin, 2018). This provides us with two token embedding distributions: longtail and baseline.

For each token embedding in the longtail distribution, we compute cosine similarity to the nearest token embedding in the baseline distribution. For each longtail image, we define the  $K$  tokens that are furthest from the the baseline distribution as longtail keywords. We retain the (description, keyword) pairs of the  $P = 40$  longtail examples per class whose keyword tokens are furthest from the base distribution.

Following, we create  $P = 40$  refined prompts per class by prompting GPT-4o (OpenAI, 2023) with: *<VLM description of the image> The following keywords describe the key features of the description above: <Keyword 1>, <Keyword 2> ... Use a complete sentence to summarize the key features. The sentence should start with: A photo of <Class> that...*

Example (image, keyword) pairs are displayed in Figure 8 of the main paper. Example refined prompts are displayed in Table 6. We emphasize that not all keywords found by this method are immediately meaningful (e.g. satin as in *satin-like pedals*, ether as in *ethereal appearance*, but they can be quickly scanned for longtail themes and, quantitatively, the process improves generalization performance beyond manual prompt tuning.

A photo of a bearded iris that showcases its deep purple petals with a yellow and brown pattern running through the <b>underside</b> , set against a blurred background to emphasize the flower’s texture and color.
A photo of sweet pea that showcases a <b>young</b> plant with a single, unfurled green leaf and a small, green flower bud beginning to open, set against a softly blurred green background, highlighting the delicate texture and promise of the flower to come.
A photo of red ginger that showcases a vibrant red flower with a yellow center, surrounded by slightly <b>damaged</b> green leaves, set against a blurred natural background.
A photo of morning glory that showcases vibrant petals with a gradient from deep red to blue-purple, arranged in a spiral pattern, with smooth texture and <b>dew</b> droplets, set against a blurred background to emphasize the flower’s intricate details and colors.

Table 6. Example refined prompts generated by Longtail Introspection for Flowers data. Keywords are **bolded**.

#### A.4. Dataset Details

We summarize each dataset used in Table 7. Additional details can be found in the (Zhang et al., 2023b) for Caltech, Cars, Pets, and Flowers or (Du et al., 2024) for ImageNet-100, ImageNet-A, and ImageNet-V2 variants. Notably, (Du et al., 2024) creates evaluation subsets of ImageNet-A and ImageNet-V2 that overlap with the training classes of ImageNet-100, listed in Figure 10. For fair comparison, we also train on ImageNet-100 and evaluate on the ImageNet-100 (Eval), ImageNet-A, and ImageNet-V2 subsets as defined in (Du et al., 2024). We emphasize that these datasets exhibit example counts that are common for longtail data in production settings.

Dataset	Classes	#Train	#Val	#Synthetic
Caltech101	102	3060	6084	61200
Cars	196	8144	8041	162880
Flowers	102	6557	1632	131140
Pets	37	3680	3669	110400
ImageNet-100	100	129860	5000	100000
ImageNet-A*	41	-	1852	-
ImageNet-V2*	100	-	10000	-
ImageNet-LT	1000	115846	20000	24000

Table 7. Overview of datasets with number of classes, training samples, validation samples, and synthetic samples. \*ImageNet-A and ImageNet-V2 are not trained on; they are only used for evaluation.

n01498041	n01514859	n01582220	n01608432	n01616318	n01687978	n01776313	n01806567	n01833805	n01882714
n01910747	n01944390	n01985128	n02007558	n02071294	n02085620	n02114855	n02123045	n02128385	n02129165
n02129604	n02165456	n02190166	n02219486	n02226429	n02279972	n02317335	n02326432	n02342885	n02363005
n02391049	n02395406	n02403003	n02422699	n02442845	n02444819	n02480855	n02510455	n02640242	n02672831
n02687172	n02701002	n02730930	n02769748	n02782093	n02787622	n02793495	n02799071	n02802426	n02814860
n02840245	n02906734	n02948072	n02980441	n02999410	n03014705	n03028079	n03032252	n03125729	n03160309
n03179701	n03220513	n03249569	n03291819	n03384352	n03388043	n03450230	n03481172	n03594734	n03594945
n03627232	n03642806	n03649909	n03661043	n03676483	n03724870	n03733281	n03759954	n03761084	n03773504
n03804744	n03916031	n03938244	n04004767	n04026417	n04090263	n04133789	n04153751	n04296562	n04330267
n04371774	n04404412	n04465501	n04485082	n04507155	n04536866	n04579432	n04606251	n07714990	n07745940

Figure 10. List of ImageNet-100 Classes trained and evaluated on as defined by (Du et al., 2024)

#### A.5. Can We Continuously Mine for Additional High-Value Synthetic Data?

Dataset	Caltech	Cars	Flowers	Pets	Avg
LTG (100 epoch)	71.5	85.1	90.9	82.0	82.4
LTG (200 epoch)	72.9	85.4	92.6	82.1	83.3
LTG (300 epoch)	72.9	85.4	92.6	82.2	83.3

Table 8. Top-1 Accuracy when training with Longtail Guidance for many epochs.

In Table 8 we ask: if Longtail Guidance generates high-value training data for predictive model  $f_\phi$ , can we continuously iterate between fine-tuning  $f$  and generating synthetic data for additional generalization improvements? In this experiment, we generate synthetic data according the original schedules defined in Table 5 for the first 100 epochs. We then continue fine-tuning and generating an additional  $1\times$  expansion every 5 epochs for a total of 300 epochs and report generalization performance. We observe that in all cases, we can improve performance, but that gains eventually saturate. It remains a question for future work whether higher-capacity generative models could be mined longer periods of time before predictive performance saturates. If so, it suggests an exciting future possibility of continuously exchanging unused offline compute for improved predictive model performance.

#### A.6. Computational Costs

##### EPISTEMIC HEAD

The Epistemic Head with  $K$  heads has a parameter count equal to  $K \times d_{\text{model}} \times C$ , for model embedding dimension  $d_{\text{model}}$  and number of output logits  $C$ . For many predictive models, this leads to negligible parameter count increase, as displayed

in Table 9 – less than 5% increase for all experiments in this paper. Training and inference times are impacted by less than 2% for our most expensive (ImageNet-LT) experiments.

Classes	Epistemic Heads	
	3	5
10	0.03%	0.04%
100	0.27%	0.45%
1000	2.67%	4.44%

Table 9. Epistemic Head Parameter Count as a Percentage of ViT-B Parameter Count

## LONGTAIL GUIDANCE

We generate  $512 \times 512$  resolution synthetic images at an unoptimized rate of 6.32 image / second for baseline text-prompted diffusion and 1.01 image / second for diffusion with Longtail Guidance (using Stable Diffusion v1.4 in FP16 with 50 DDIM sampling steps on 8xH100 GPUs). The majority of the LTG guidance cost is in differentially decoding through the VAE. In particular, in the gradient

$$\frac{dz_t^0}{dz_t} \times \frac{d\hat{x}_t^0}{d\hat{z}_t^0} \times \frac{df_\phi^{\text{lt}}}{d\hat{x}_t^0} \quad (12)$$

calculated by the main paper’s Algorithm 1, the second term is VRAM-intensive (45GB for batch size 8 without gradient checkpointing). This cost occurs primarily because the 83.6m parameter VAE decodes latent dimensions of  $64 \times 64 \times 4$  to data dimension  $512 \times 512 \times 3$ .

### A.7. Longtail Signals

In Figure 11 we show that high quantiles  $q = 90\%$  of model-based longtail signals are all strong indicators of examples that are disproportionately hard for the model (as determined by average accuracy above and below the quantile). However, as shown in Figure 5 of the main paper, the Epistemic Head more effectively *detects* rare or hard examples.

In Figure 12, we visualize a toy example of high epistemic (left) and high aleatoric (right) uncertainty for three Epistemic Heads each classifying over three classes. High epistemic uncertainty occurs when each sample from the predictive posterior (i.e. each Epistemic Head) gives mutually incompatible answers (such as all being confident about a different class). High aleatoric uncertainty (which includes high entropy) occurs when each sample has similarly and highly ambiguous (e.g. uniform) belief over classes.

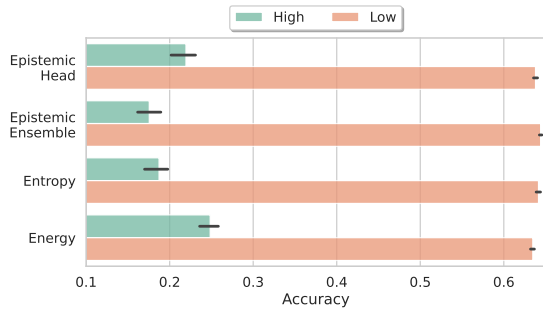


Figure 11. High quantiles of longtail signal indicate examples that are disproportionately hard.

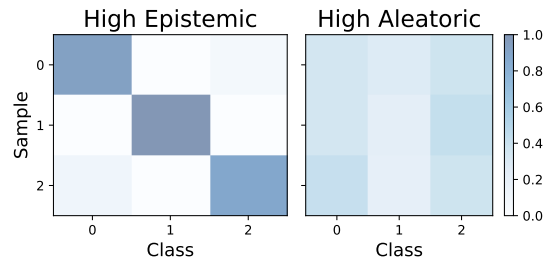


Figure 12. Probability of classification under high epistemic and high aleatoric uncertainty. There are three samples from the posterior predictive (y-axis). Each maintains a distribution over three classes (x-axis). Epistemic uncertainty (left) goes high when each sample has mutually incompatible beliefs. Aleatoric uncertainty (right) goes high when samples are all highly uncertain.



### A.8. Why Does Longtail Guidance Work without Training the Predictive Model on Intermediate Diffusion States?

A key finding and contribution of this work is that an existing predictive model  $f_\phi$  does not need to be retrained on intermediate, noisy diffusion states to effectively guide diffusion model  $\epsilon_\theta$  towards high-value synthetic training examples that are rare or hard from  $f$ 's perspective. This realization frees us from the dilemma of having to decide whether to waste predictive model capacity training on intermediate diffusion data it will never see in production or risking divergence from the production model by fine-tuning on intermediate noisy states. But why does this work?

In Figure 13, we visualize the intermediate, noisy diffusion states of two quantities: the decoded, predicted terminal state  $D(P(\hat{x}_t^0))$  (top row, what LTG uses as guidance input to predictive model  $f_\phi$ ) and the decoded data state,  $D(x_t)$  (bottom row, what classifier guidance would traditionally perform guidance if not in a latent space). We observe that the terminal state predictions much more readily resemble natural image data at a much earlier time in the diffusion process (within the first 10% of denoising steps) than do the data states. In fact, decoded data states have off-distribution noise artifacts up through the first 90% of the diffusion denoising steps.

We make this quantitative with the Frechet Inception Distance (FID) (Heusel et al., 2017), defined as

$$\text{FID} = \|\mu_r - \mu_g\|^2 + \text{Tr}(\Sigma_r + \Sigma_g - 2(\Sigma_r \Sigma_g)^{\frac{1}{2}}) \quad (13)$$

where  $(\mu_r, \Sigma_r), (\mu_g, \Sigma_g)$  are the mean and covariance of Inception-V3's pool3 features for real and synthetic data, respectively. Lower FID indicates that the generated data more closely match and cover the real data. We measure FID for two conditions:

1. FID between the decoded, predicted terminal state  $\hat{x}_t^0 = D(P(x_t))$  and real ImageNet-LT training data, and
2. FID between the decoded data state  $x_t$  and real ImageNet-LT training data.

Results are plotted in Figure 15. Observe that the decoded, predicted terminal state  $D(P(\hat{x}_t^0))$  are dramatically closer (in distribution) to real training data than are the naively decoded data states,  $x_t$  for nearly all denoising iterations.

Figure 14 demonstrates that, because the terminal state estimates  $D(P(\hat{x}_t^0))$  are closer real training data, the predictive model is able to effectively guide data generations towards higher longtail signals (model entropy in this case), with clear longtail signal separation between different longtail guidance weights occurring within the first 25% of denoising iterations. In contrast, naively guiding based on data states  $x_t$  causes the predictive model to be unable to effectively guide data generation until the last 5% of denoising iterations, when there are no longer many degrees of freedom for the diffusion model to meaningfully change image content.

### A.9. Ablations

In Table 16, we ablate over Longtail Guidance signal (energy, entropy, epistemic) by Longtail Guidance Weight (1.0, 10.0, 50.0, 200.0) for the Pets dataset. In Table 17, we ablate over the number of Epistemic Heads on the same task. In both cases, we report predictive model generalization performance when trained on the  $30\times$  synthetic data expansion task as defined in Section 4.1. We find highest performance for energy and entropy at guidance weight 10.0 and highest performance for epistemic at guidance weight 50.0. Similarly, we find highest performance for  $K = 5$  Epistemic Heads. Performance declines with additional heads, likely because the oracle loss used to train the Epistemic Head causes each head to be exposed to  $\frac{1}{K}$  examples in expectation; too many heads and they lose the ability to represent the predictive model.

### A.10. Additional Examples

In Figure 18, we show high-resolution examples of synthetic data generated by baseline diffusion and by Longtail Guidance. In order, classes are: jellyfish, flamingo, lion, monarch butterfly, ant, candle, jeep, forklift, and ambulance. Guidance is performed by a SOTA ViT-based ImageNet-LT classifier described in Supplement A.1.

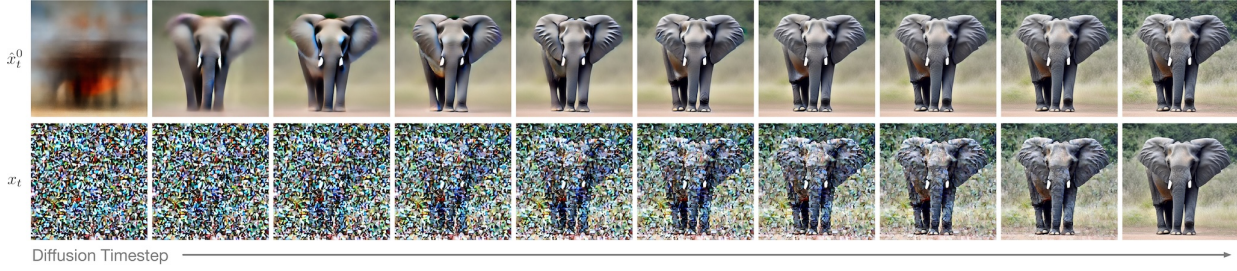


Figure 13. Performing Longtail Guidance on predicted, decoded terminal states  $\hat{x}_t^0$  (top row) provides production model  $f_\phi$  with data that are more in-distribution and less corrupted by intermediate diffusion noise than does Naive guidance performed on each intermediate decoded state  $x_t$  (bottom row). See Figures 14, 15 for quantitative analysis.

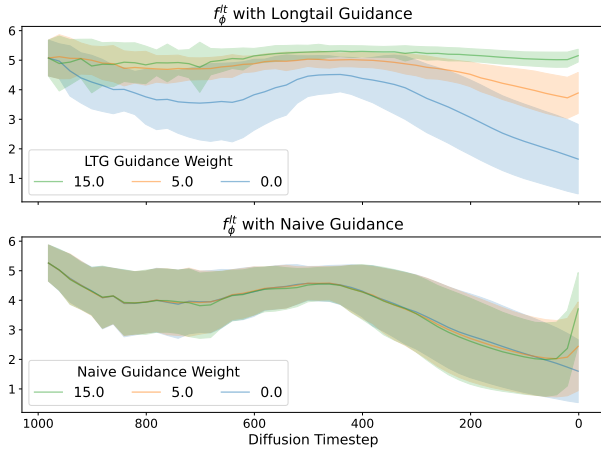


Figure 14. Performing Longtail Guidance on the predicted, decoded terminal data state  $\hat{x}_t^0$  (top row) provides production model  $f_\phi$  with cleaner data much earlier in the diffusion denoising process, enabling it to meaningfully exercise guidance as compared to naively performing guidance on the predicted decoded data state  $x_t$ . Y-axes are the guiding model longtail signal (in this case, entropy). See Figure 13 for a visual depiction.

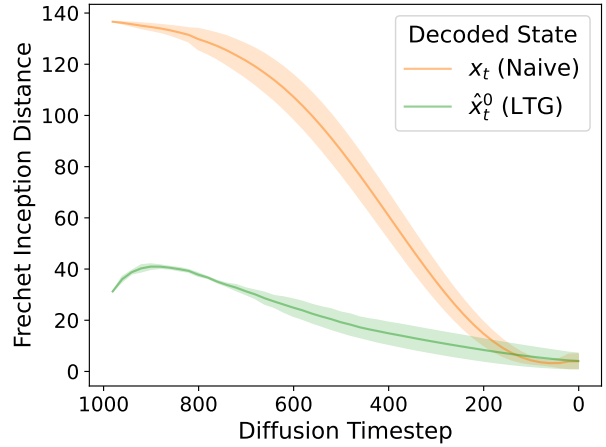


Figure 15. Decoded terminal data states  $\hat{x}_t^0$  have better FID with respect to real training data than do intermediate data states  $x_t$ , suggesting that LTG works with an existing predictive model  $f_\phi$ , even though it is not trained on intermediate diffusion states, precisely because the states upon which LTG performs guidance better match what the predictive model has already seen.

Longtail Signal	Longtail Guidance Weight			
	1.0	10.0	50.0	200.0
Energy	78.8	<b>80.0</b>	78.9	76.7
Entropy	76.1	<b>81.6</b>	80.9	74.9
Epistemic	76.8	78.5	<b>82.0</b>	79.1

Figure 16. Ablation over Longtail Guidance Weight on Predictive Model Generalization Performance on the Pets Dataset Expansion Task, holding the number of Epistemic Heads fixed at  $K = 5$ . Entries are bolded for best hyperparameter in each row.

Epistemic Heads	3	5	7	9
LTG (Epistemic)	81.2	<b>82.0</b>	80.6	79.9

Figure 17. Ablation over Epistemic Heads on Predictive Model Generalization Performance on the Pets Dataset Expansion Task, holding the guidance weight fixed at 50.0.



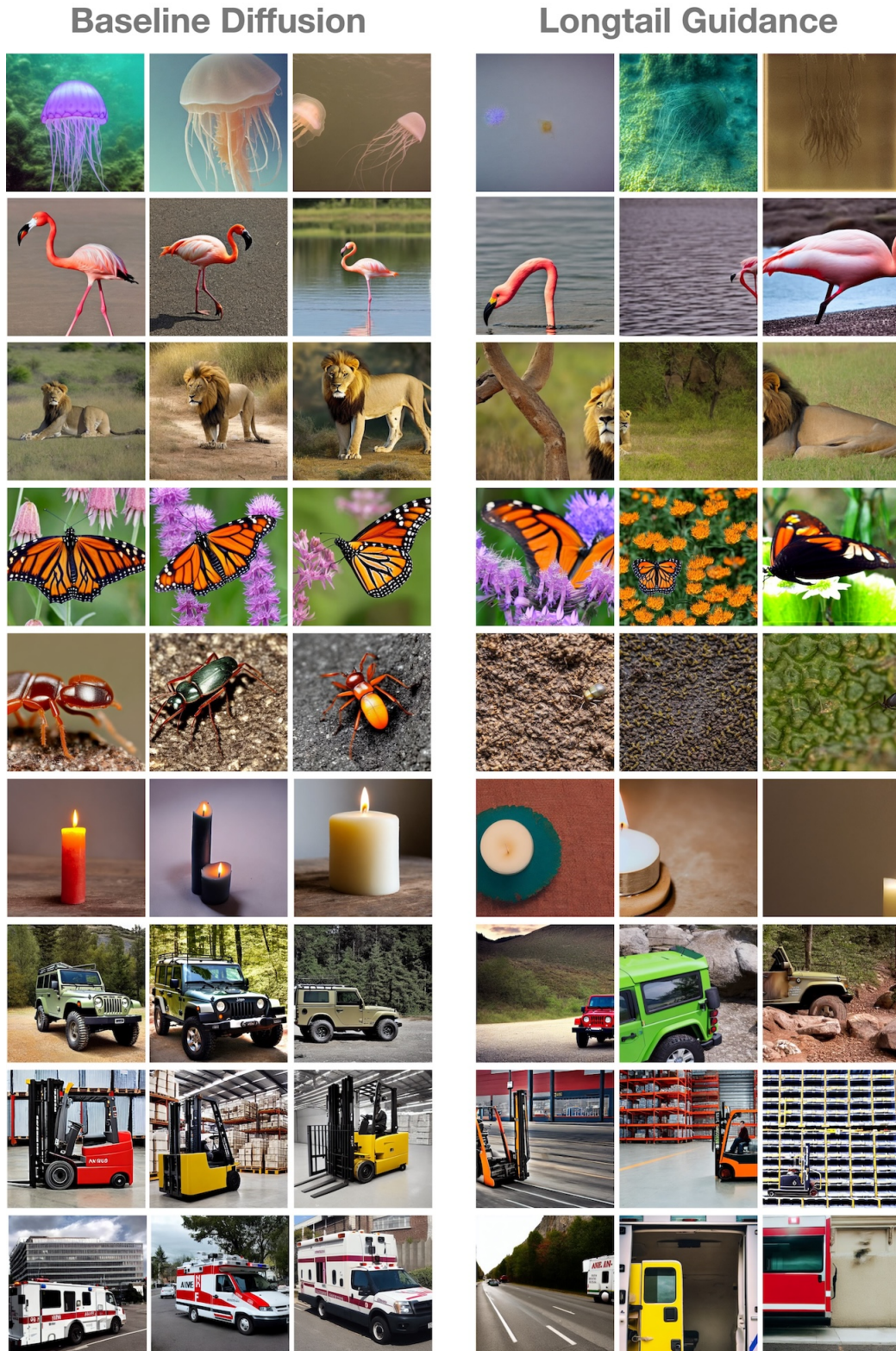


Figure 18. Additional example of baseline diffusion (left) and Longtail Guidance (right). Baseline diffusion tends to generate canonical, well-posed views that help a predictive generalize, but only up to a point. In contrast, Longtail Guidance produces more extreme, occluded, or challenging views from the perspective of a predictive model, enabling significantly improved generalization performance.